CLIMATE EXTREME INDICES OVER ITALY

EVAN DAVID WELLMEYER
M.Sc. Atmospheric Science and Technology
Course in Climate Modeling
Dr. Gianluca Redaelli
Dr. Lorenzo Sangelantoni
Università Degli Studi Dell'Aquila, L'Aquila
Sapienza Università Di Roma, Rome

2022

1 Introduction

Climate in a narrow sense is usually defined as the average weather, or more rigorously as the statistical description in terms of the mean and variability of relevant quantities over a period of time ranging from months to thousands or millions of years [1]. The classical period for averaging these variables as defined by the World Meteorological Organization (WMO) is 30 years thus defining the climatological normal [2].

Climate change refers to change in the state of the climate identified by changes in the mean and/or the variability of its properties and that persists for an extended period, typically decades or longer. These changes can be attributed to natural internal processes or external forces such as modulations of the solar cycle, volcanic eruptions and persistent anthropogenic changes to the composition of the atmosphere or the land use. The United Nations Framework Convention on Climate Change (UNFCCC) defines climate change as the change of climate which is attributed directly or indirectly to human activity that alters the composition of the global atmosphere which is in addition to natural climate variability observed over comparable time periods [3].

Climate change is a global phenomenon, and while it is often referred to publicly and politically through global average temperature change, the real manifestation and consequence of climate change are very different across regions of the earth [4]. With every increment of global warming, changes get larger in regional mean temperature, precipitation and soil moisture [5]. This makes it essential to define risk assessments and climate impact on the subcontinental to local scale [4]. Regional climate change refers to a change in climate in a given region identified by changes in mean or higher moments of the probability distribution of a climate variable and persisting for a few decades or longer [4]. One of the biggest representations of a changing global climate is seen in climate extremes. The occurrence of a value of a weather or climate variable above (or below) a threshold value near the upper (or lower) ends of the range of observed values of the variable are called climate extremes [3]. These extremes can be assessed through climate extreme indices produced from the outputs of climate models.

Global Climate Models (GCMs) are dynamical models that provide climate projections at a global scale by numerically solving prognostic equations in a global Eulerian framework. GCMs can be earth system models (ESMs), coupled atmosphere-ocean general circulation models (AOGCMs) or atmosphere-only general circulation models (AGCMs). Operating resolutions of GCMs allow little information to be extracted regarding climate changes in specific regions. Regional Climate Models (RCMs) can act as a nested domain inside a GCM operating at a higher resolution. RCMs are forced at the lateral boundaries from GCMs without feeding back into the GCM (one-way nesting); however, this means RCMs can inherit biases from GCMs in addition to producing biases themselves. RCMs can also be run with inputs from multiple model types covering a wide range of spatial scales and processes. RCMs have many limitations, some of which include the neglecting air-sea coupling of cloud-aerosol interaction which can influence the regional climate projections. However, latest generation RCMs couple additional components such as with the ocean and aerosols in order to produce more accurate projections as well as the investigation of additional climate processes.

The temporal evolution of a climate system towards a future state is called a pathway [3]. In order for climate models to predict future climate scenarios, assumptions must be made based on socio-economic and physical states and/or changes to the system that affect the pathway. Representative Concentration Pathways (RCPs) are a method of representing the socio-economic and physical status within a climate system in order to define the amount of anthropogenic forcing considered in climate projections. RCPs do this by specifying concentrations of greenhouse gases (GHGs) that will result in total radiative forcing increasing by a specified amount by the year 2100 in relation to pre-industrial levels. Radiative forcing targets are measured in watts per

square meter (W m^{-2}) total radiative forcing at the top of the atmosphere and are defined at 2.6, 4.5, 6.0 and 8.5 W m^{-2}. Shared socio-economic pathways (SSPs) were developed to complement RCPs by implementing into the models climate adaptation and mitigation efforts. The SSPs describe alternative socio-economic futures in the absence of climate policy, compromising sustainable development (SSP1), regional rivalry (SSP3), inequality (SSP4), fossil-fueled development (SSP5), and a middle-of-the-road development (SSP2) [3].

2 Materials and methodology

The Coordinated Regional climate Downscaling EXperiment (CORDEX) provides ensembles of high resolution historical and future climate projections for various regions of the globe. RCMs in CORDEX typically have a horizontal resolution ranging from 50 to 10 km.

This study assesses changes regarding climate extreme indices over the Italian peninsula. Outputs of three regional climate models at approximately 12 km resolution from the Euro-Cordex initiative for the periods 1971-2000 and 2071-2100 (RCP 8.5) driven by the ERAint Global Climate Model (GCM) produced by ECMWF. The RCMs include the Royal Netherlands Meteorological Institute (KNMI) Regional Atmospheric Climate Model (RACMO); the Danish Meteorological Institute (DMI) HIRHAM model, an RCM combining aspects of HIRLAM and ECHAM models; and the Swedish Meteorological and Hydrological Institutes (SMHI) Rossby Centre Regional Atmospheric Climate Model (RCA4).

An algorithm written in Shell scripting, using Climate Data Operator (CDO) and NCO programming languages was provided by the professor and was edited to produce the climate extreme indices considered in this study.

Climate indices considered include consecutive summer days index (CSU), highest one day precipitation amount (RX1) and consecutive dry days (CDD) index. The CSU index measure the maximum number of consecutive days where the maximum temperature is greater than 25.0 C and CDD index is a measure of the maximum number of consecutive days with less than 1 mm of precipitation occurring.

The graphical post-processing of this study was done in Matlab, where plots were produced showing the historical period, the future period, and the difference between the them for the two climate extreme indices. Time series' of the relevant variables spatial average were also produced and subsequently applied linear and quadratic fitting using relevant Matlab tools.

3 Results and Discussion

From the climate data extracted from the EURO-CORDEX, results were obtain from the maximum temperature at the surface (tasmax) and precipitation (PR) outputs to which subsequent climate extreme indices were applied.

3.1 Temperature

A time series showing outputs for tasmax from the three models considered is shown in Figure 1, along with the model ensemble mean. The three models resulted very similar for the tasmax variable, with SMHI-RCA4 model resulting with the highest values toward the end of the future period and KNMI-RACMO having slightly lower values than the rest of the ensemble for the later half of the future period. The DMI-HIRHAM model was very close to the ensemble mean for the future period. A linear fit applied to the ensemble mean resulted in a slope of 0.037, with r-square = 0.966 and RMS = 0.36. The quadratic fit result was better for the tasmax variable with r-square = 0.98 and RMS = 0.27.

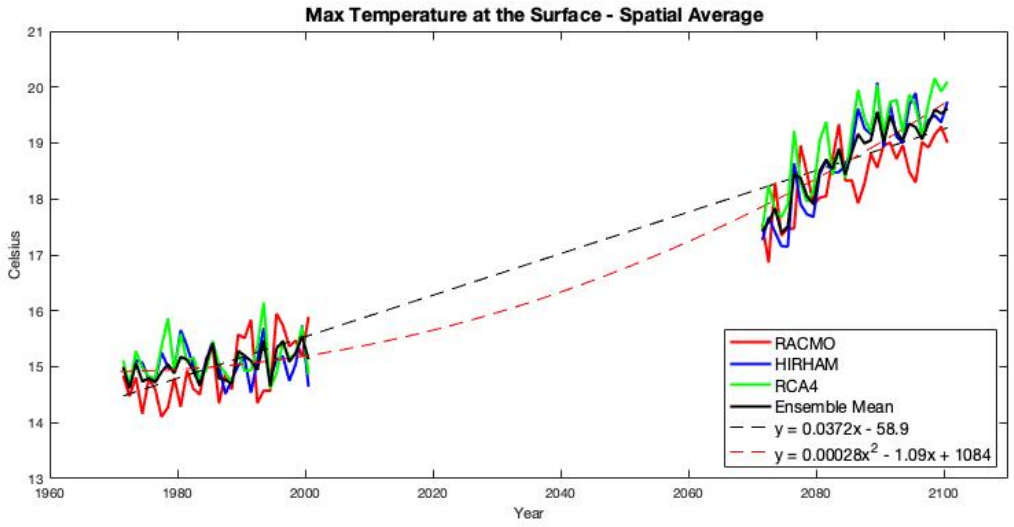

Figure 1: Spatial average of maximum temperature at the surface (tasmax) for the ensemble with linear and quadratic fit.

3.1.1 Consecutive Summer Days Index (CSU)

The temporal average for the consecutive summers days (CSU) index from each model are shown in Figures 2 and 3 with the difference between future and reference in Figure 4. Outputs for the reference period (Figure 2) show no significant difference between KNMI-RACMO22E and DMI-HIRHAM5 models, with SMHI-RCA4 showing elevated reference levels; however, these are in spatial accordance with the former two models.

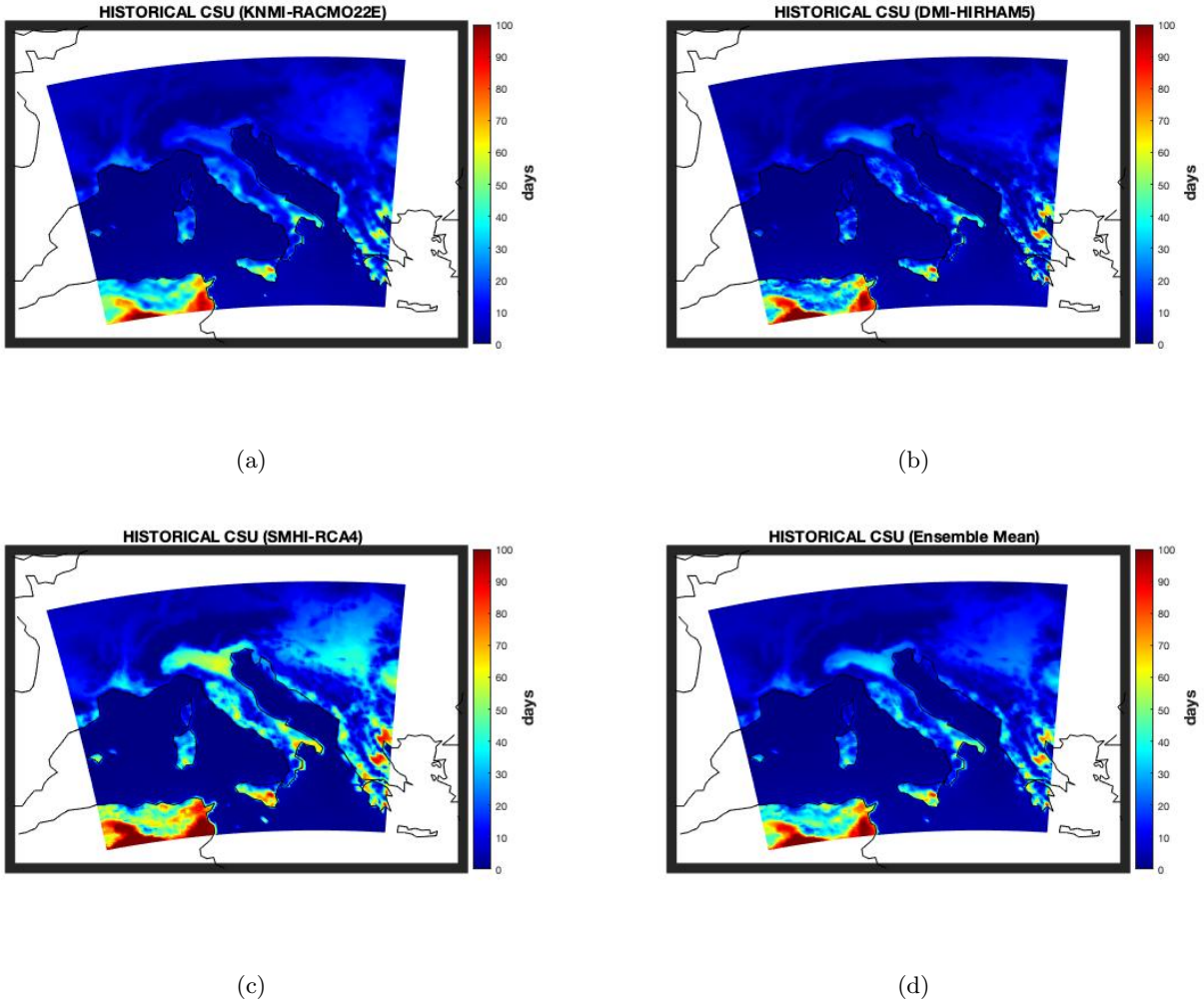

(a) (b)

(c) (d)

Figure 2: Mean signal of Consecutive Summer days index (CSU) for the historical (reference) period 1971-2000 from the three regional climate models with ensemble mean.

Temporal averages of the CSU index for the future period (Figure 3) shows significant difference between the three models in terms of magnitude, with SMHI-RCA4 showing the largest values for CSU followed by DMI-HIRHAM5 and then KNMI-RACMO22E. The three models are spatially in accordance over the domain. As expected with reference to the tasmax timeseries (Figure 1), the ensemble mean closely resembles the output from the DMI-HIRHAM5 model.

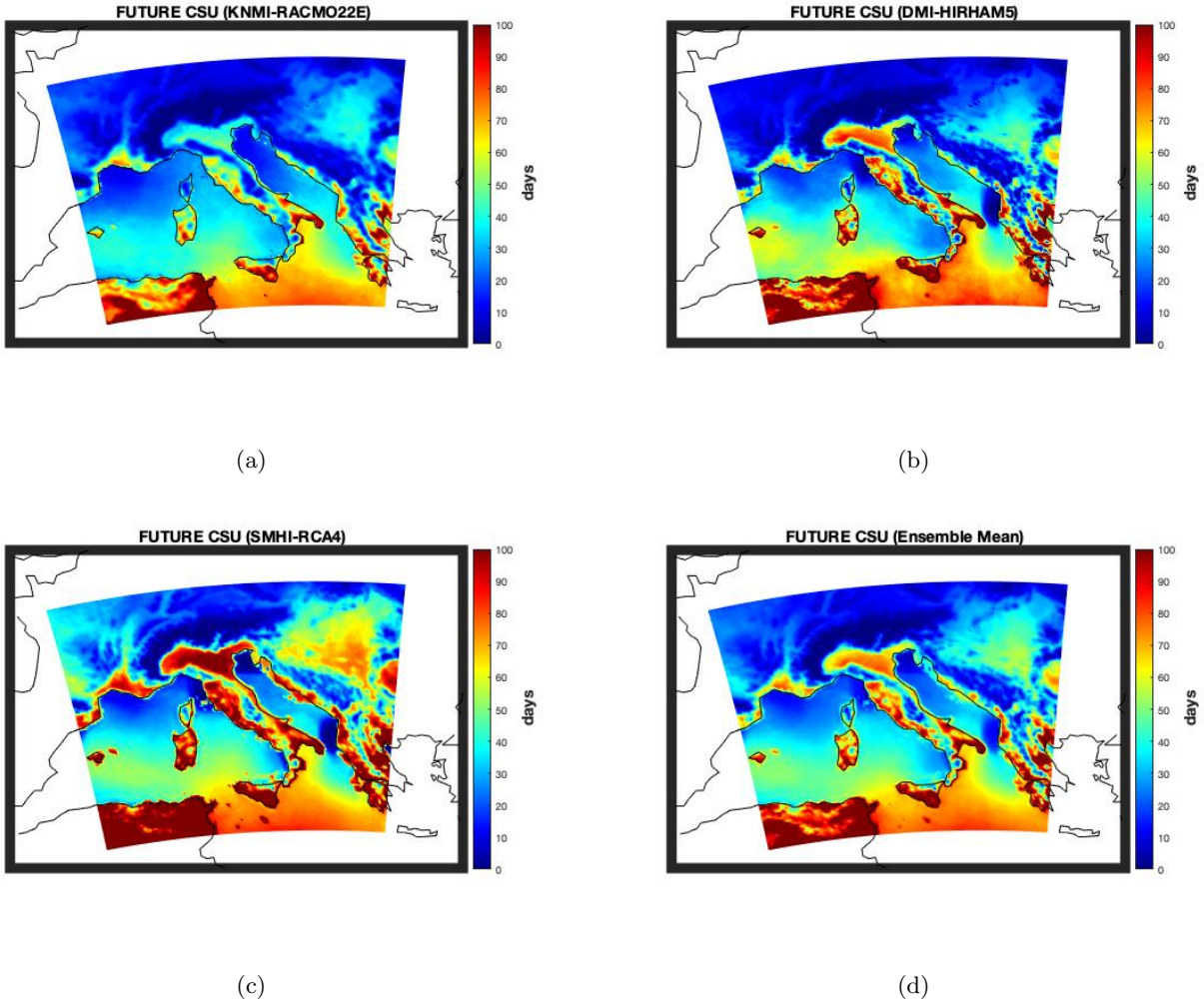

(a) (b)

(c) (d)

Figure 3: Mean signal of Consecutive Summer days index (CSU) for the future period 2071-2100 from the three regional climate models with ensemble mean.

The difference between the mean signals from the future period and the reference period (Figure 4) show the three models evolved quite differently. The KNMI-RACMO22E model shows small differences across most of the domain, with the largest increase across the bottom of the domain in the Mediterranean sea, with an increase of 60-70 CSU and an increase of 30-50 CSU across parts of Italy. The DMI-HIRHAM5 model shows larger increases in CSU than the KNMI-RACMO22E model, with the largest increases still present at the bottom of the domain of 70-90 CSU; however, larger increases in CSU are present throughout Italy with approximately 80 CSU increase in parts of Sicily, and 50-80 CSU up the western coast of Italy. A notable difference between the DMI-HIRHAM5 model and the KNMI-RACMO22E model is in the Po Valley region, with DMI-HIRHAM5 showing a significantly larger increase in CSU compared to that of KNMI-RACMO22E. The SMHI-RCA4 model is similar to the other two models in showing the largest difference in CSU across the bottom of the domain in the Mediterranean sea; however, spatially the differences are less isolated across the rest of the domain, with almost all of Italy showing a 40-50 CSU increase. In the case of the CSU, the ensemble mean signal shows an appropriate balance between the models in both spatial distribution and in magnitude, with the largest increases in CSU mostly appearing in the coastal areas and through the Po Valley.

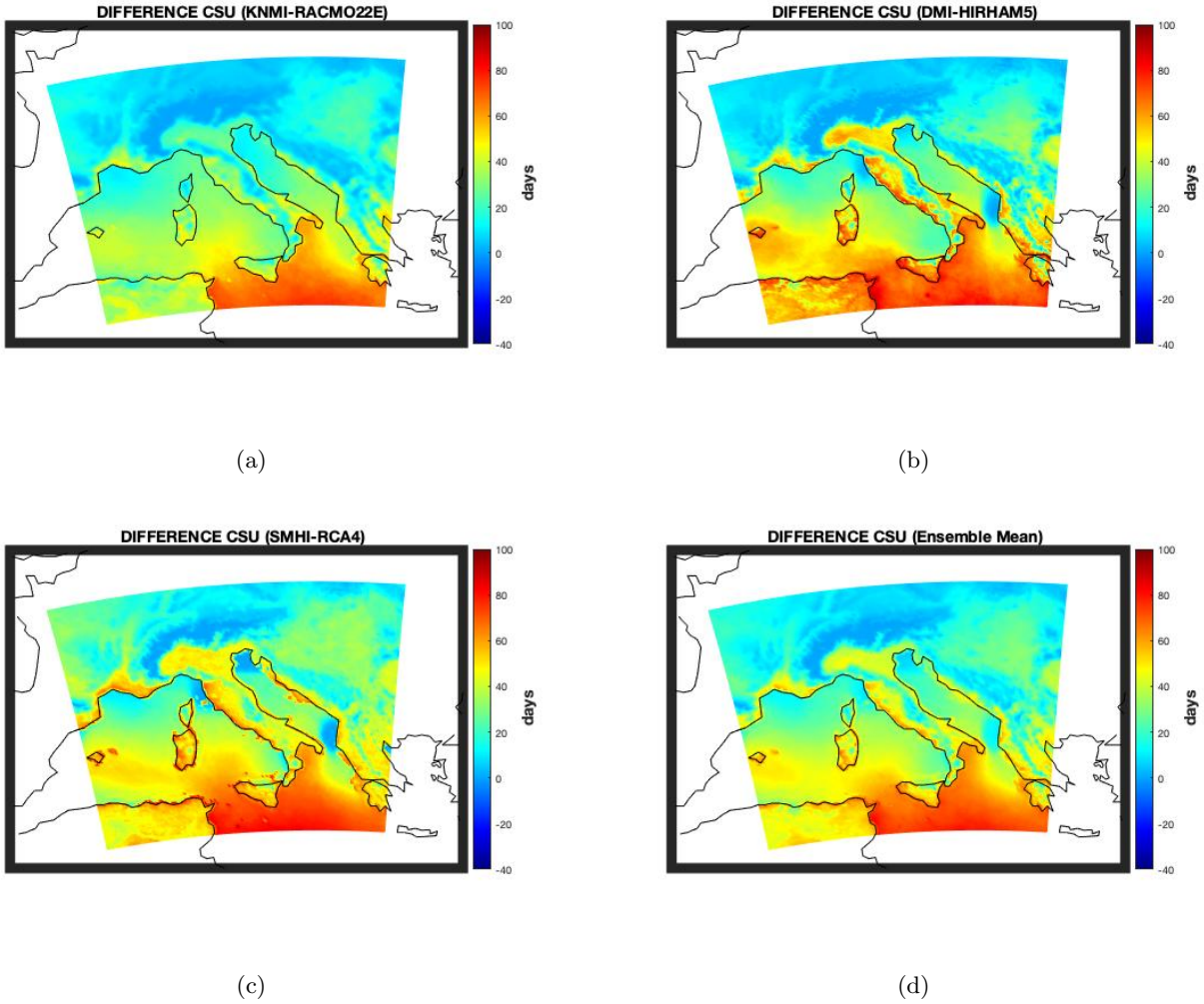

(a) (b)

(c) (d)

Figure 4: Difference in mean signal for Consecutive Summer days index (CSU) of the future period (2071-2100) and the historical (reference) period 1971-2000 from the three regional climate models with ensemble mean.

The spatial average of the mean signal for the three modes of the three models are shown in Figure 5, showing all models averaged 8-15 CSU over the reference period and between 35 and 55 CSU over the future period, giving a difference of approximately 28-38 CSU for the three models. In terms of temporal and spatial average, the models behaviors are very similar to each other.

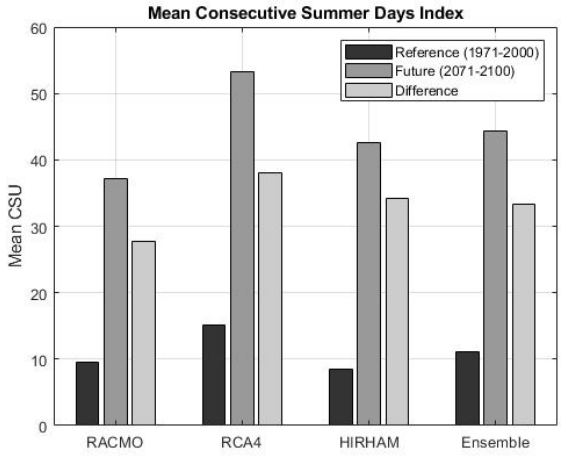

Figure 5: Spatial and temporal mean signal of the ensemble for the three cases.

The timeseries for the ensemble average of the CSU index is shown in Figure 6. The linear fit applied to the

ensemble average resulted in a slope of 0.34, with r-square = 0.92 and RMS = 5.12. The quadratic fit of the CSU timeseries was slightly better with r-square = 0.95 and RMS 4.00.

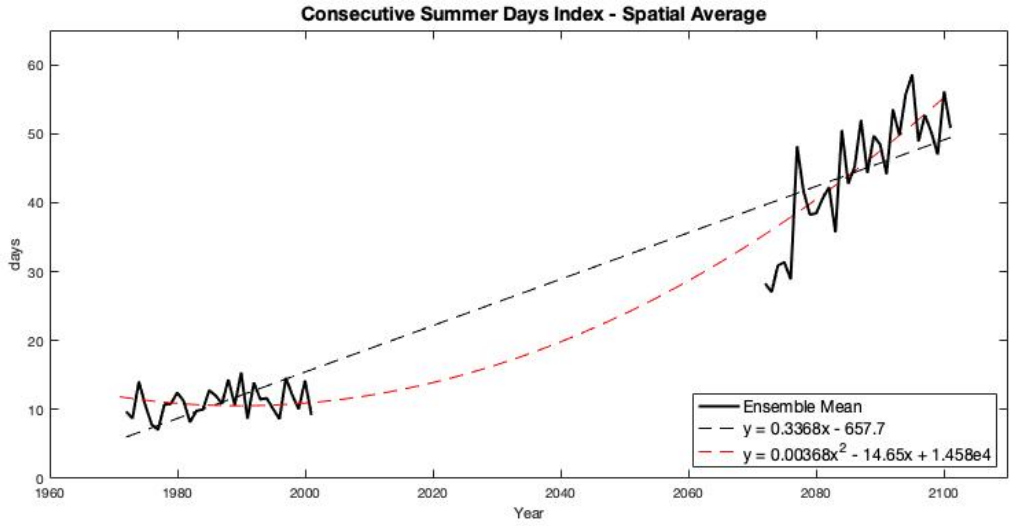

Figure 6: CSU trend

3.2 Precipitation

A time series showing outputs for precipitation from the three models considered is shown in Figure 7, along with the model ensemble mean. A linear fit applied to the ensemble mean resulted in a slope of -0.0013, with r-square = 0.23 and RMS = 0.13. The quadratic fit result was not significantly different for the precipitation variable with r-square = 0.25 and RMS = 0.12.

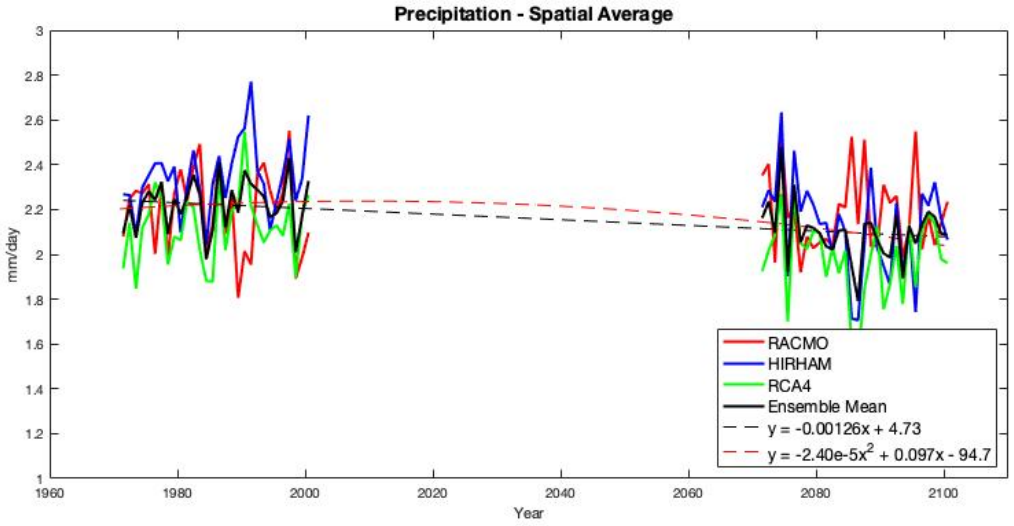

Figure 7: Spatial average of precipitation for the ensemble with linear and quadratic fit.

3.2.1 Highest One-Day Precipitation (RX1)

Averages for the mean signal of highest one day precipitation (RX1) from the reference period are shown in Figure 8. Values for the KNMI-RACMO22E and SMHI-RCA4 models are considerably higher in comparison to DMI-HIRHAM5 model for the reference period, with peak values ranging from 80-180 mm/day; however spatial distribution of peak values are in accordance across the three models. Spatial resolution appears higher for the DMI-HIRHAM5 and SMHI-RCA4 models, notably in the Alp region of northern Italy.

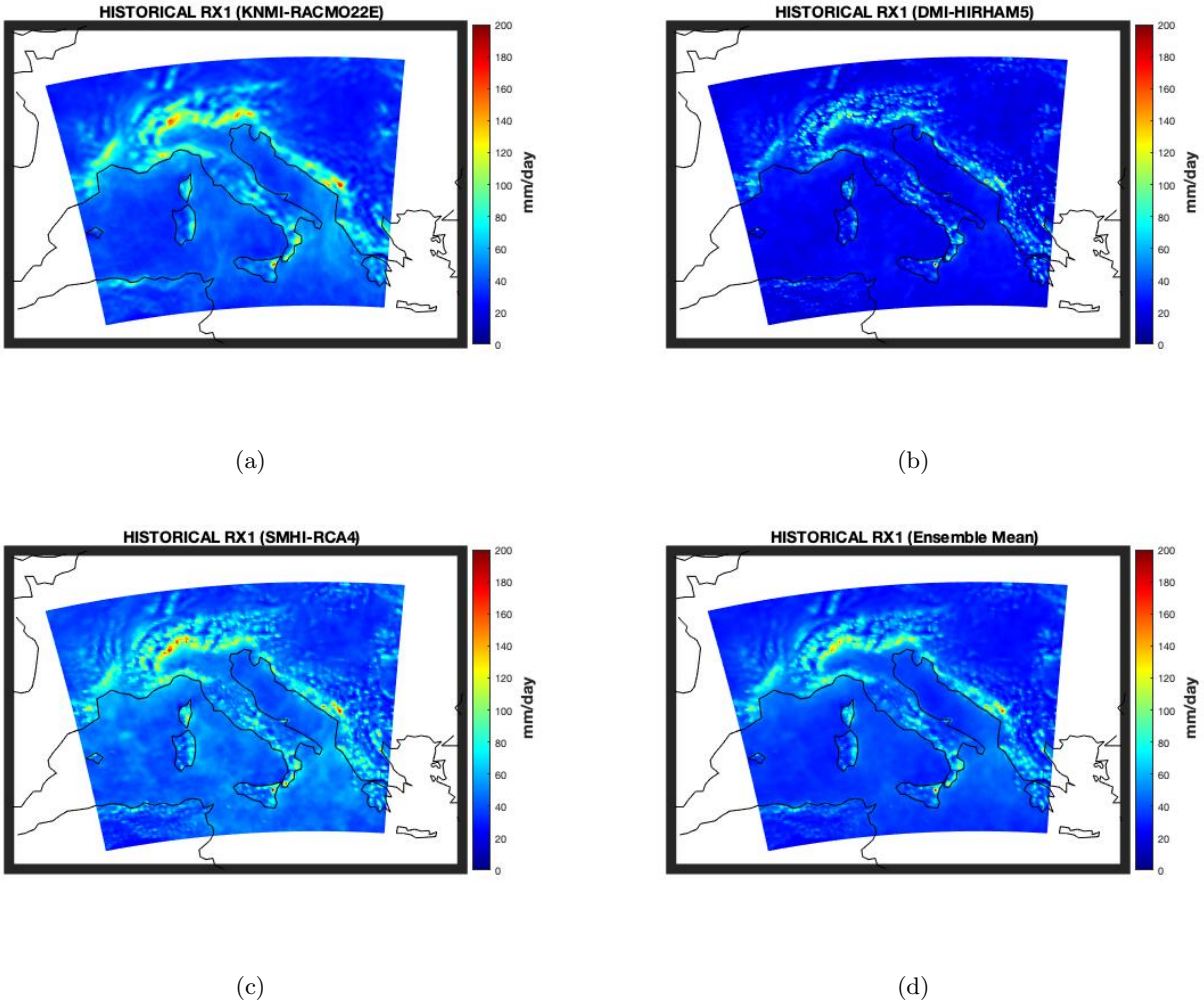

(a) (b)

(c) (d)

Figure 8: Mean signal of highest one day precipitations index (RX1) for the historical (reference) period 1971-2000 from the three regional climate models with ensemble mean.

The mean signal of RX1 of the three models for the future period is shown in Figure 9, with DMI-HIRHAM5 showing the largest values across most of the domain. The visual difference in spatial resolution between DMI-HIRHAM5/SMHI-RCA4 and KNMI-RACMO22E is even more notable with the higher values. The area of largest values in the domain for the three models is in the Alp region, as well as down the eastern Adriatic coast.

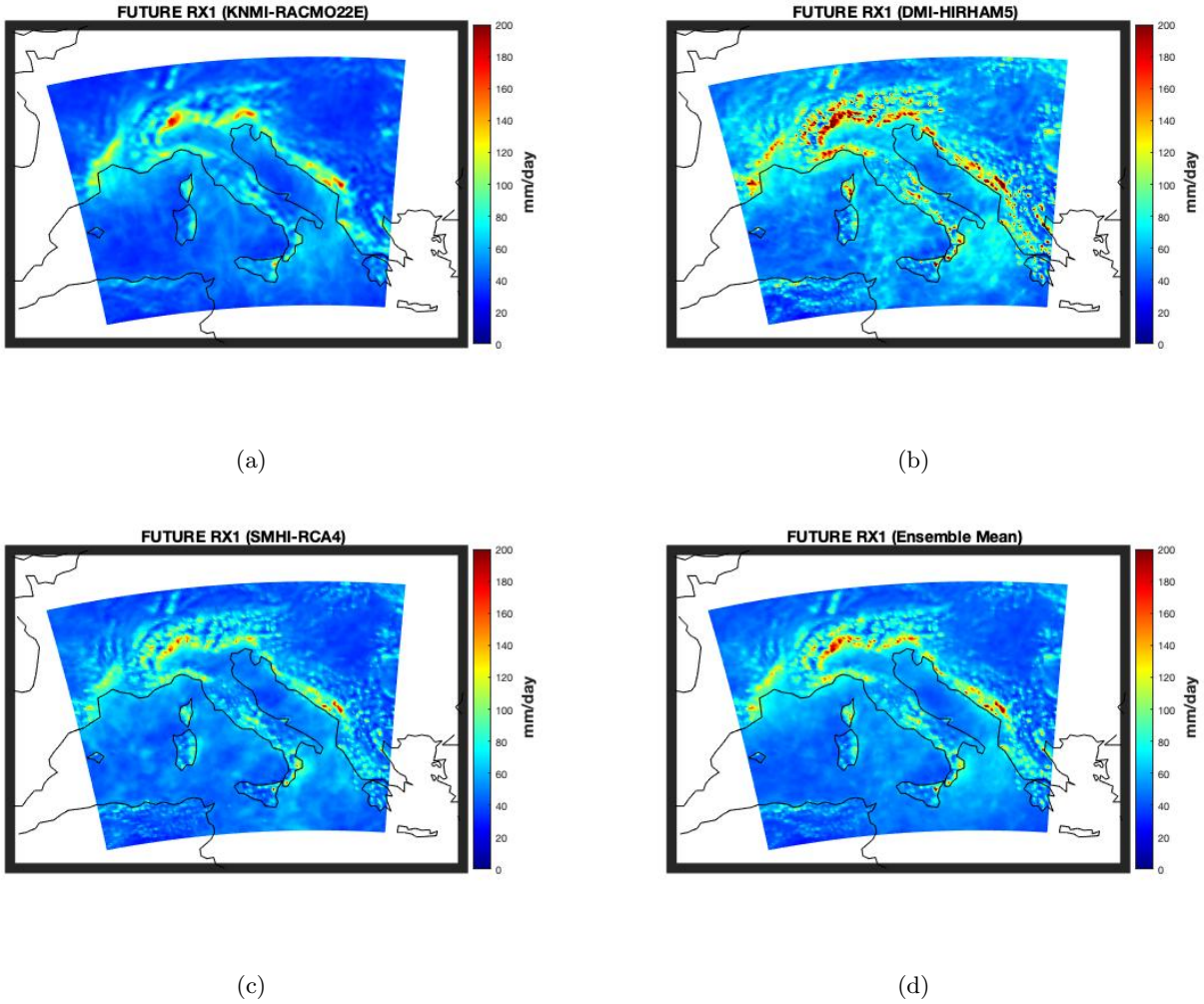

(a) (b)

(c) (d)

Figure 9: Mean signal of highest one day precipitation index (RX1) for the future period 2071-2100 from the three regional climate models with ensemble mean.

The difference in mean signals between the future and reference period for the RX1 index (Figure 10) are significantly different among the three models. DMI-HIRHAM5 shows the most appropriate difference in terms of geographical isolation of changes. The spatial distribution of changes for both KNMI-RACMO22E and SMHI-RCA4 models seems random and without physical significance to the geography of the domain. In this case the ensemble mean is important in combining the sparse result of the KNMI-RACMO and SMHI-RCA4 models with the more geographically appropriate result of the DMI-HIRHAM model.

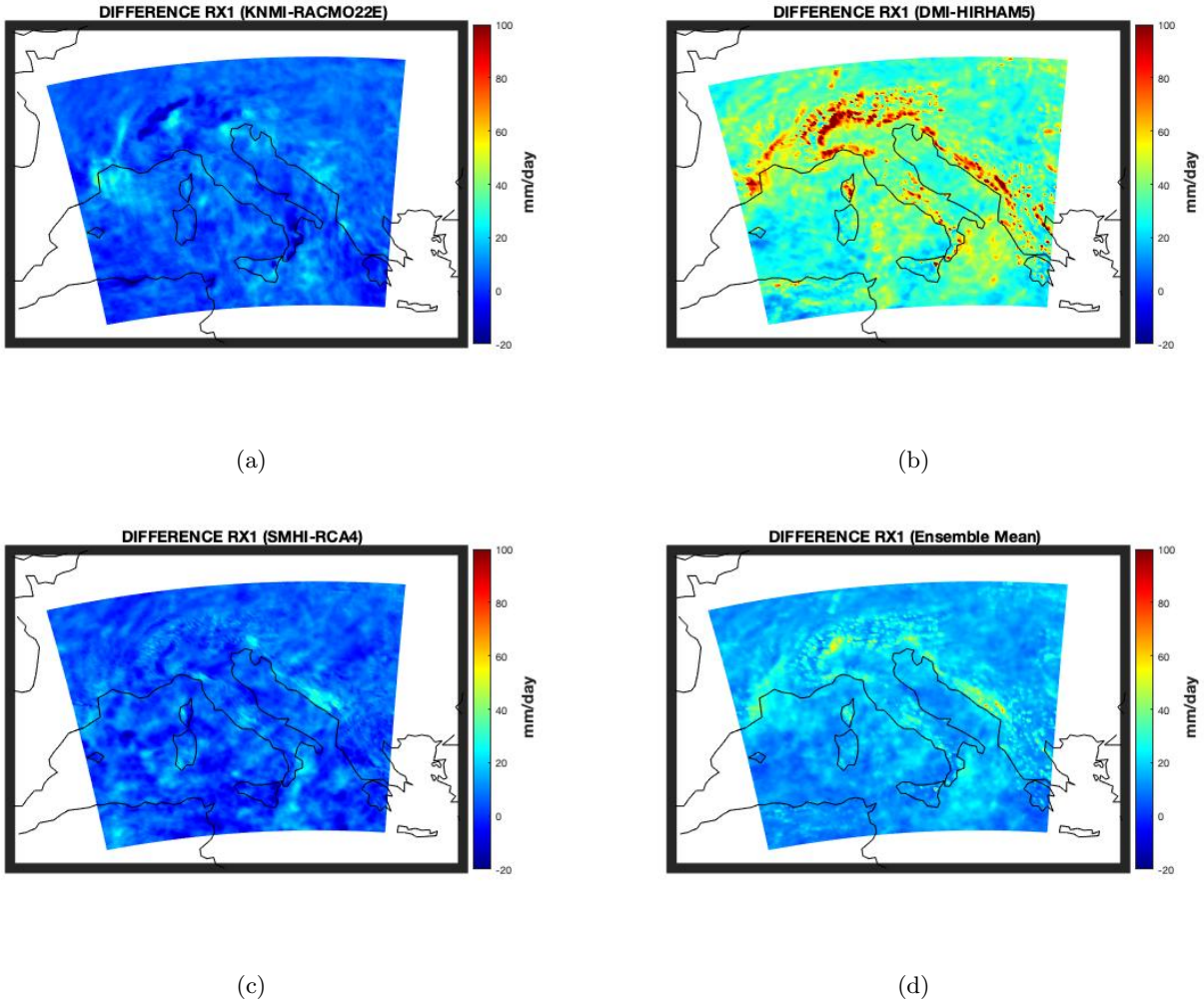

(a) (b)

(c) (d)

Figure 10: Difference in mean signal for highest one day precipitation index (RX1) of the future period (2071-2100) and the historical (reference) period 1971-2000 from the three regional climate models with ensemble mean.

The spatial average of the RX1 mean signal for the three modes of the three models are shown in Figure 11. There is a significant difference across the models with KNMI-RACMO22E and SMHI-RCA4 showing the largest reference mean, and the smallest difference between the future and reference periods. DMI-HIRHAM5 continues to show the more physical result with difference of approximately 35 mm between the future and reference periods.

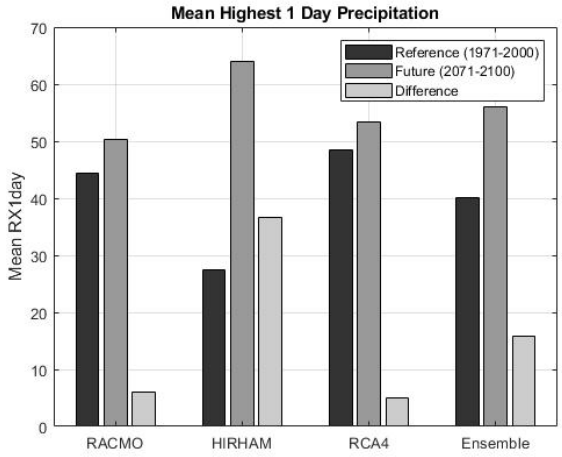

Figure 11: Spatial and temporal mean signal of highest one day precipitation index for the ensemble in the three cases.

The timeseries for the RX1 ensemble mean is shown in Figure 12. Due to large differences in magnitude among the three models, only the ensemble mean is shown. A linear fit resulted in a slope of 0.015 with r-square = 0.89 and RMS = 2.81. The quadratic fit (not shown) applied to the ensemble mean showed negligible difference to that of the linear fit.

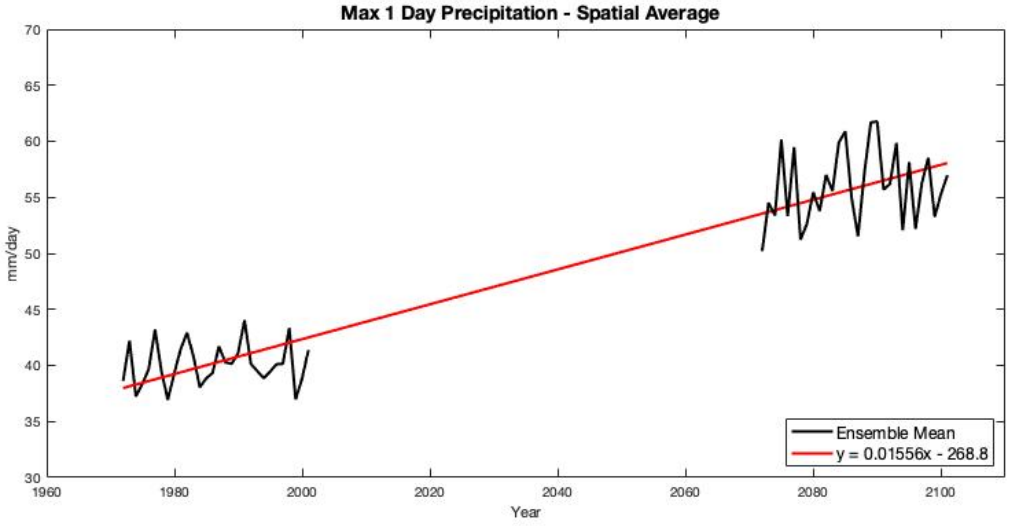

Figure 12: Spatial average of highest one day precipitation for the ensemble with linear fit.

3.2.2 Consecutive Dry Days index (CDD)

The mean signal of CDD for the three models from the reference period are shown in Figure 13. The KNMI-RACMO22E model appears to differ from the other two models in terms of how it handles the difference between land/sea surfaces, as it shows considerably higher values for CDD over the sea when compared to the other two models. Spatial distribution of CDD values is comparable between models over the land areas, with KNMI-RACMO22E and SMHI-RCA4 showing 40-50 CSU in southern Italy and DMI-HIRHAM5 showing slightly less. Ensemble mean signal is useful in this case in combining the differing aspects of the models outputs.

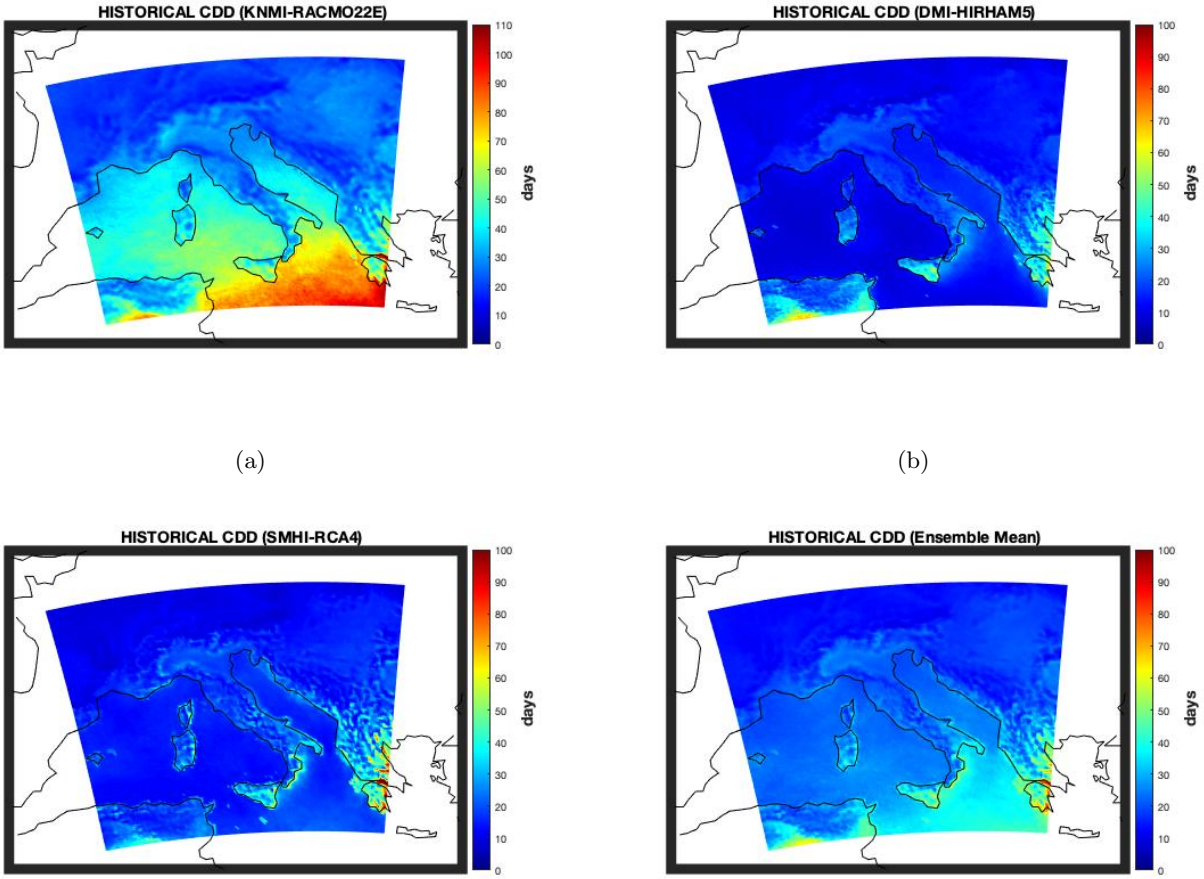

(a) (b)

(c) (d)

Figure 13: Mean signal of the consecutive dry days index for the reference period from the three models with ensemble mean.

The mean signal of CSU for the future period (Figure 14) shows the same distinction between KNMI-RACMO22E and the other two models. With DMI-HIRHAM5 and SMHI-RCA4 showing more physically consistent results. Additionally, there is a notable difference of apparent resolution from the SMHI-RCA4 model in terms of geographically isolated peaks in the CSU values. Ensemble mean signal shows values similar to that of the DMI-HIRHAM model over the land areas with the addition of elevated values in the Mediterranean area provided from the KNMI-RACMO model.

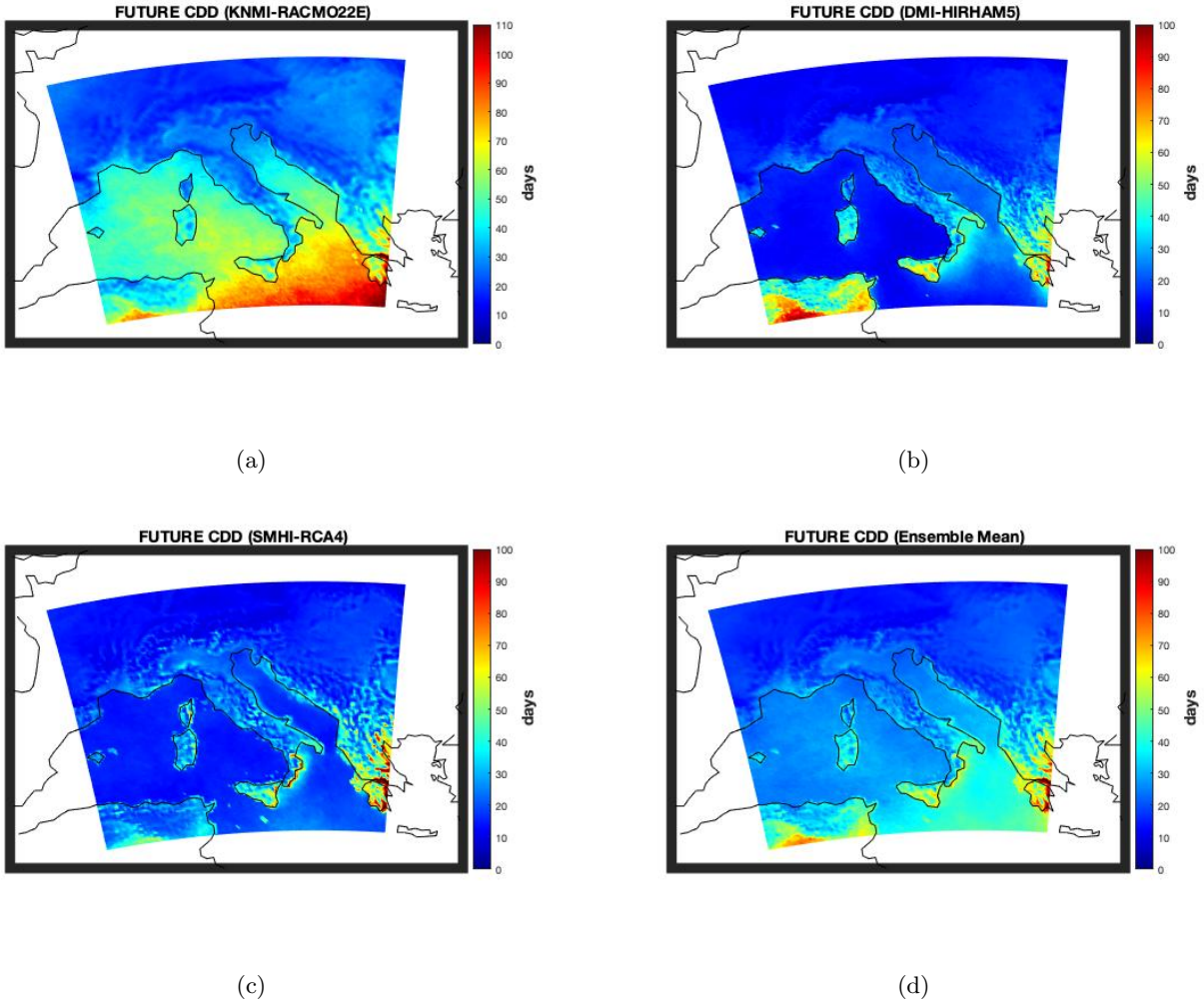

(a) (b)

(c) (d)

Figure 14: Mean signal of the consecutive dry days index for the future period from the three models with ensemble mean.

The difference in mean signals between the future and reference periods for the three models are shown in Figure 15. Due to the diversity between the KNMI-RACMO22E and the other two models, the difference greatly illuminates how the models compare. The DMI-HIRHAM5 model shows large increases in CSU in southern Italy with smaller increases up the western coast and in Sardinia. SMHI-RCA4 likewise shows increases in CSU but with more geographical isolation. The KNMI-RACMO22E model shows large increases in CSU to the west of the domain, with no noticeable geographical relevance to the result with the exception of the Alpine region.

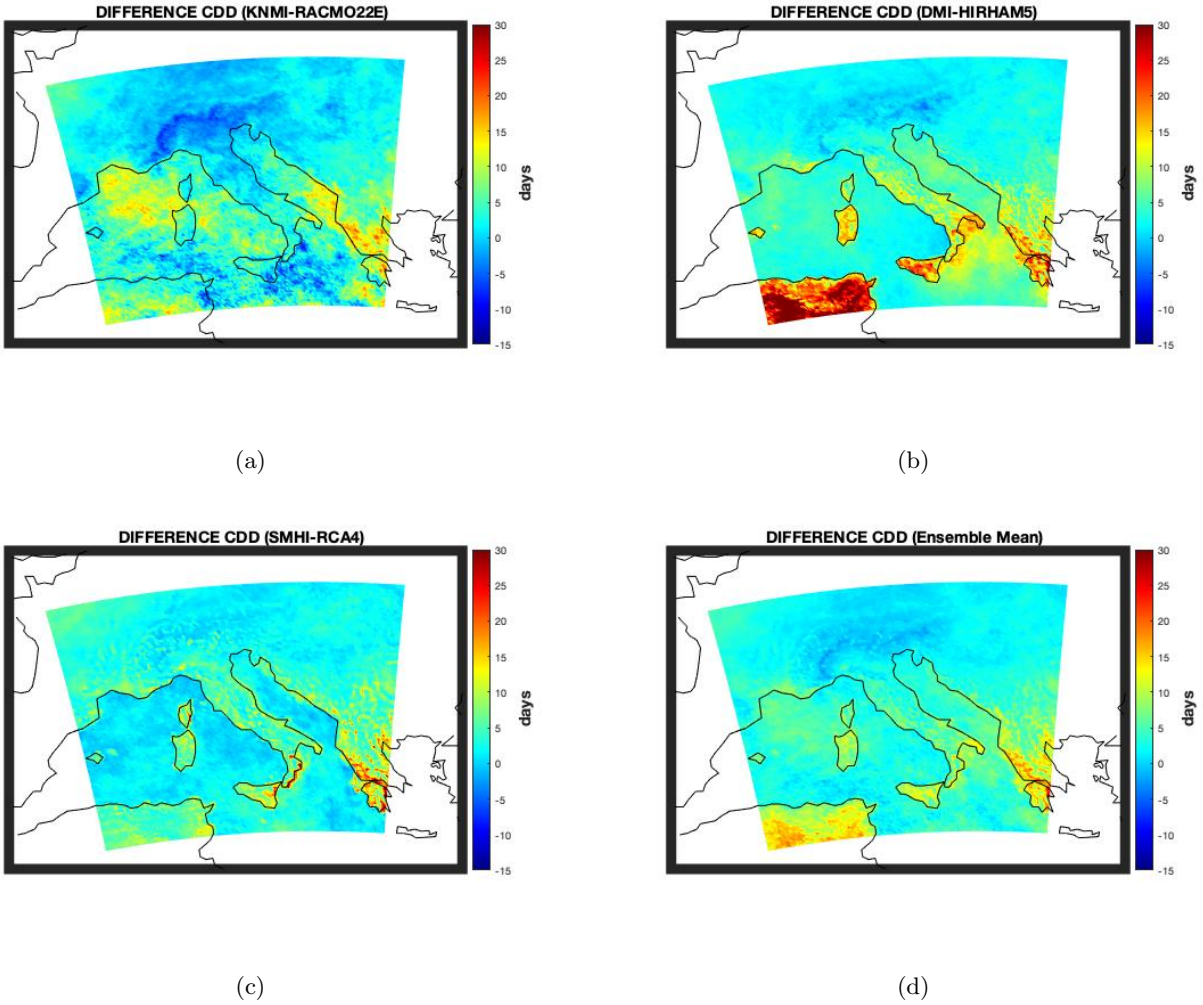

(a) (b)

(c) (d)

Figure 15: Difference in CDD mean signal between future and reference periods for the three models with ensemble mean.

The spatial average of the mean signal for the three modes of CDD is shown in Figure 16. There is a large difference in magnitude between the KNMI-RACMO22E model and the other two models. SMHI-RCA4 and DMI-HIRHAM5 models are comparable in magnitude for both periods, with DMI-HIRHAM5 showing a slightly larger increase in CDD between the future and reference periods at approximately 25 days.

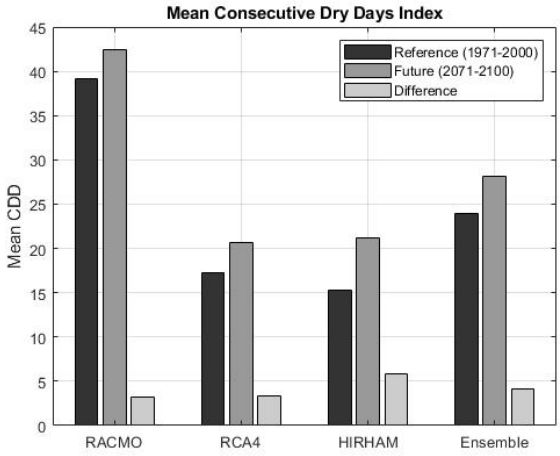

Figure 16: Spatial and temporal average of the mean signal for consecutive dry days index for the three models and three modes.

The timeseries of CDD for the ensemble mean is shown in Figure 17. Once again due to differences in magnitude, the individual model timeseries' are not shown. The ensemble mean does however show massive swings in CDD through the years for both historic and future periods. The linear fit resulted in a slope of 0.042, with r-square = 0.38 and RMS = 2.73. The quadratic fit (not shown) applied to the CDD ensemble mean showed negligible difference to that of the linear fit.

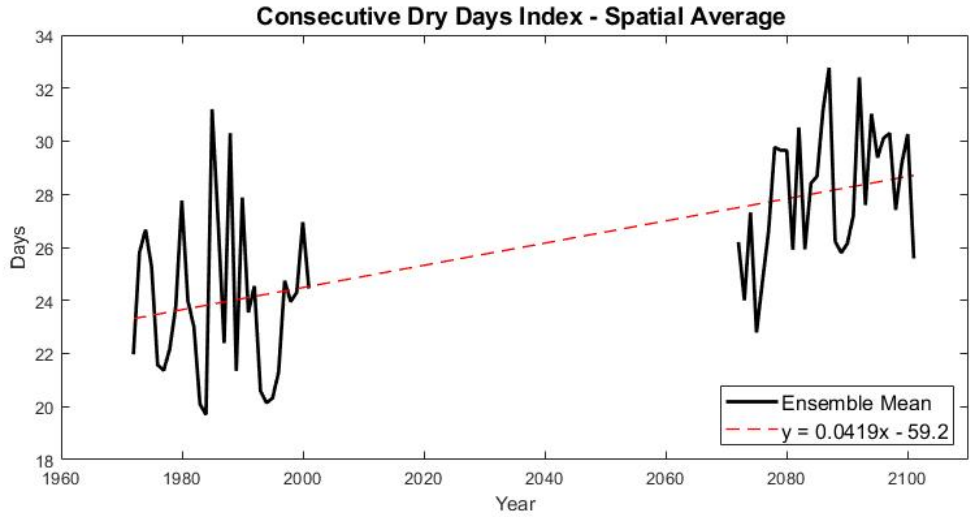

Figure 17: Time series of the model ensemble mean for consecutive dry days index with linear fit.

3.3 Discussion

Changes to the global climate has dire consequences to the every component of the earth system and the organisms that live there. The IPCC Sixth Assessment Report (AR6) puts the present increase of global mean surface temperature (GMST) at 1.09°C for the 2011-2020 period compared to the 1850-1900 pre-industrial baseline [6]. While not all regions of the globe evolve the same under these global warming conditions, the climate extreme indices considered in this report emphasize the effects that a few degrees of change in GMST can have on regional climates beyond simple changes in temperature. The consecutive summer days index from all models considered show that the temperature changes displayed in the temperature and CSU timeseries' are not distributed evenly across the domain, that some local areas will experience dramatic changes to their seasons to which a cascade of consequences can occur. Looking at changes in the climate beyond temperature, the consecutive dry days index shows us that some regions could experience an increase of 10-15 consecutive days without rain, to an average CDD of 50-60 days in some areas. Large periods of drought like this would have severe consequences on the agriculture of the regions, and additionally those who depend on it, as well as other organisms that will not survive though such periods. The highest one day precipitation index shows us that despite precipitation slightly decreasing on average into the future period, that the intensity of the rains that are observed would increase dramatically, leading to unprecedented flooding–an effect we may already be experiencing considering the recent flooding events in Italy. This effect is elevated when considering extreme rain events occurring on top of an increase in consecutive dry days.

4 Conclusion

Despite the changes in GMST of 1.09°C seeming insignificant to some. We see that if the earths climate system continues to evolve at the current rate, significant consequences will incur across many (if not all) aspects of the climate system in different regions of the globe. The max temperature at the surface and precipitation outputs extracted from the EURO-CORDEX for the models DMI-HIRHAM5, KNMI-RACMO22E and SMHI-RCA4 for the future period 2071-2100 with reference period 1971-2000 at RCP8.5 show clear insight into these changes on the regional scale through climate extreme indices. Those indices considered show longer summers, more intense rains and longer periods of drought.

In summery, the RCMs used performed well considering the representative concentration pathway of focus and highlighted changes to the climate system of the Italian peninsula through climate extreme indices via Climate Data Operator command tools. While RCP8.5 is the projection considering the highest amount of anthropogenic forcing, it is a clear signal as to the fate of the climate system if significant changes in anthropogenic emissions of GHGs are not made.

References

[1] IPCC. *Climate Change 2022: Mitigation of Climate Change. Contribution of Working Group III to the Sixth Assessment Report of the Intergovernmental Panel on Climate Change*. Cambridge University Press, Cambridge, UK and New York, NY, USA, 2022.

[2] K. Dinse. Climate variability and climate change. 05 2014.

[3] IPCC. *Annex I: Glossary*, page 541–562. Cambridge University Press, 2022.

[4] I.O. Adelekan E. Totin A. Ayanlade J. Efitre A. Gemeda K. Kalaba C. Lennard C. Masao Y. Mgaya G. Ngaruiya D. Olago N.P. Simpson Trisos, C.H. and S. Zakieldeen. *Chapter 10: Linking Global to Regional Climate Change*, pages 1285–1455. Cambridge University Press, 2022.

[5] Sarah Connors, Micheline Dionne, Gábor Hanák, Rade Musulin, Neil Aellen, Muhammad Amjad, Steven Bowen, Daniel Ruiz Carrascal, Erika Coppola, Eric Moro, Alessandro Dosio, Sergio Faria, Thian Yew Gan, Melissa Gomis, J. Gutiérrez, Pandora Hope, Robert Kopp, Svitlana Krakovska, Katherine Leitzel, and Xuebin Zhang. *Climate Science: A Summary for Actuaries - What the IPCC Climate Change Report 2021 Means for the Actuarial Profession*. 03 2022.

[6] IPCC. *Climate Change 2022: Impacts, Adaptation, and Vulnerability. Contribution of Working Group II to the Sixth Assessment Report of the Intergovernmental Panel on Climate Change*. Cambridge University Press, Cambridge, UK and New York, NY, USA, 2022.